

# Evidence for an extended scattered disk.

B. Gladman<sup>1</sup>, M. Holman<sup>2</sup>, T. Grav<sup>3</sup>,  
J. Kavelaars<sup>4</sup>, P. Nicholson<sup>5</sup>, K. Aksnes<sup>3</sup>, J-M. Petit<sup>1</sup>

<sup>1</sup>Observatoire de la Côte d'Azur, France

<sup>2</sup>Harvard-Smithsonian Center for Astrophysics, USA

<sup>3</sup>University of Oslo, Norway

<sup>4</sup>McMaster University, Canada

<sup>5</sup>Cornell University, USA

Proposed running head: Evidence for an extended scattered disk.

Submitted to Icarus, Mar 26/2001

Keywords: Kuiper Belt, trans-neptunian objects, comets.

22 text pages + 4 figures + 2 tables = 28 pages in initial submission

## Abstract

By telescopic tracking, we have established that the orbit of the trans-neptunian object (2000 CR<sub>105</sub>) has a perihelion of  $\simeq 44$  AU, and is thus outside the domain controlled by strong gravitational close encounters with Neptune. Because this object is on a very large, eccentric orbit (with semimajor axis  $a \simeq 216$  AU and eccentricity  $e \simeq 0.8$ ) this object must have been placed on this orbit by a gravitational perturbation which is *not* direct gravitational scattering off of any of the giant planets (on their current orbits). The existence of this object may thus have profound cosmogonic implications for our understanding of the formation of the outer Solar System. We discuss some viable scenarios which could have produced it, including long-term diffusive chaos and scattering off of other massive bodies in the outer Solar System. This discovery implies that there must be a large population of trans-neptunian objects in an ‘extended scattered disk’ with perihelia above the previously-discussed 38 AU boundary.

# 1 Introduction

Current nomenclature commonly divides the trans-neptunian region of the solar system into (1) the ‘Kuiper Belt’ (consisting of so-called ‘classical belt’ objects and ‘resonant objects’ in various mean-motion resonances with Neptune), and (2) the ‘scattered disk’ (Jewitt *et al.* 1998). Finer distinctions and sub-populations are possible (see Gladman *et al.* 2001). The ‘scattered disk’ is a structure that was observed to form naturally in simulations of (1) orbital perturbation of comets exterior to Neptune (Torbett and Smoluchowski 1990) and (2) of the delivery of Jupiter family comets from Kuiper Belt (Duncan and Levison, 1997). This latter work found that as trans-neptunian objects (TNOs) leave the Kuiper Belt after encountering Neptune, some are scattered outward to large, long-lived external orbits rather than being passed inward to the other giant planets. The first recognized member of this population of scattered disk objects (SDOs) was 1996 TL<sub>66</sub> (Luu *et al.* 1997); since that time of order 30 have been identified (*cf.*, Trujillo *et al.* 2000), with orbits of varying quality. The semimajor axis,  $a$ , distribution of these objects has no formal upper limit in the simulations of Duncan and Levison (1997), although a distinction from the inner Oort cloud becomes problematic at  $a > 1000$  AU (Duncan *et al.* 1987). The currently-known SDOs (Fig. 1) must be concentrated towards lower  $a$  due to selection biases; larger- $a$  SDOs spend smaller fractions of their time near perihelion where they appear brightest and are more easily detected; a bias towards small perihelion distance  $q$  will also exist.

Objects scattered to large orbits by Neptune will return to near the planet at sub-

sequent perihelion passages. For a scattered object the gravitational perturbation from Neptune might be considered as an impulse as the object passes its perihelion; this alters the velocity of the object but not its position. Thus, the  $q$ 's of scattered objects generally remain small, maintaining the possibility of encounters with the planet. Levison and Duncan (1997, Fig. 6) show that except for some cases in the 2:1 resonance with  $a \simeq 49 \text{ AU}$ , objects with  $q > 40 \text{ AU}$  are entirely absent, or at least are of extremely low probability. Some objects have their perihelia raised from 35 to  $\sim 39 \text{ AU}$  due to a phenomena of 'resonance sticking', to which we will return below. There is as yet no firm definition for the boundary between the SDOs and Centaurs, nor even between the SDOs and the rest of the Kuiper Belt (Gladman 2001). Trujillo *et al.* (2000) seem to *define* the SDO population as that with  $q=34\text{--}36 \text{ AU}$ . We note in Figure 1 growing evidence for a  $q \simeq 35\text{--}37 \text{ AU}$  'gap' in the SDO perihelion distribution, although statistics are still small and assumptions in the orbits may still be important because many of the SDO orbits are still not well sampled at time.

Once on scattered orbits, SDOs are subject to dynamical erosion as they are eventually perturbed by Neptune back onto orbits geometrically crossing that planet's orbit. Then they are either (rarely) ejected by Neptune, or have their perihelia pushed down to Uranus or below at which point their dynamical lifetimes become  $\sim 10 \text{ Myr}$ . At that point they are usually rapidly removed from the solar system (Dones *et al.* 1996, 1997, Levison and Duncan 1997). Nevertheless, the state with  $q > 30 \text{ AU}$  but still near Neptune can be very long-lived due to the long orbital periods and the low probability of Neptune being close when the object's rapid perihelion passage occurs. Torbett (1989) and Torbett and

Smoluchowski (1990) explored the long-term gravitational stability of such large- $a$  orbits with  $q$  near Neptune. They showed that such orbits could be dynamically chaotic up to  $q \simeq 45$  AU, for large semimajor axes. Although this chaotic evolution is not a sufficient condition for orbital instability (*cf.* Gladman 1993), it is in good agreement with later long-term numerical integrations in the regime of common exploration (out to about  $a=50$  AU) (Duncan *et al.* 1995). However, the time scale for orbital instability is not established; a chaotic orbit at high  $a$  may require longer than 5 Gyr to reach a state where it begins to interact strongly with Neptune. Thus, large- $a$  orbits with  $q > 38$  AU are only weakly unstable to the gravitational perturbations of the current giant planets over the lifetime of the solar system. Later, we shall expand on some details of the above broad discussion in the context of our observational result.

## 2 Observations

The object 2000 CR<sub>105</sub> was discovered on 6 February 2000 in an on-going survey by Millis *et al.* (2000), and, based on the observed 3-week arc from a second night's observations on 27 February, the Minor Planet Center (MPC) placed it on a provisional 'scattered orbit' with  $a=82$  AU,  $e=0.59$ , and  $i=31^\circ$ , implying  $q=33.8$  AU. The semimajor axis was chosen to be similar to that of 1996 TL<sub>66</sub> (B. Marsden, 2000, private communication). Since the estimated heliocentric distance at the time of discovery was  $\simeq 55$  AU, we realized this object was potentially of exceptional interest; only the much fainter 1999 DG<sub>8</sub> (Gladman *et al.* 2001), at 62 AU, had ever been discovered at such a large heliocentric distance. Thus, we re-observed 2000 CR<sub>105</sub> on 28 and 29 March 2000 at the Canada-France Hawaii 3.5-m

telescope; given the short time interval since the previous observation, we were stunned to find the object already a dramatic 24 arcseconds off the ephemeris — an enormous positional error for a trans-neptunian object. This implied that the object was moving eastward much more rapidly than indicated by the initial orbit and thus had a much larger semimajor axis. Based on these observations, the orbit was revised by B. Marsden to  $a=675$  AU,  $e=0.94$ ,  $i=23^\circ$ , making it the largest scattered disk orbit known. Even with this preliminary orbit the perihelion ( $q=41$  AU) had risen out of the region believed to be strongly coupled to Neptune, but given a two-month arc on an orbital period of greater than 10,000 yr, this perihelion distance was still rather uncertain. A further recovery attempt by M. Holman *et al.* in May 2000 at Kitt Peak failed in bad weather, after which 2000 CR<sub>105</sub> disappeared behind the Sun until November 2000.

At this point there was a broad range of possible orbits for 2000 CR<sub>105</sub>. Its astrometry was still formally consistent, within observational errors, with a parabolic orbit corresponding to a returning Oort cloud comet (albeit with the most distant perihelion ever observed). At the extreme end there was even the possibility that the orbit was hyperbolic (corresponding to the first observed interstellar comet), although this was less likely. It was still possible that CR<sub>105</sub> would turn out to have  $q < 39$  AU and a relatively ‘typical’ scattered disk orbit, but with a large semimajor axis. Lastly, and most interestingly, if a  $q > 40$  AU perihelion could be confirmed then, we believed at the time, this object would turn out to be the first SDO beyond the dynamical influence of the giant planet system.

We thus decided to allocate considerable telescope time to the recovery and orbit determination of this object, beginning in the dark run of November 2000 and continuing

every dark run until February 2001, to provide a high-quality data set on which to base orbit calculations. The first recovery was obtained with the European Southern Observatory’s 2.2m telescope on 24 and 25 November 2000, followed a few days later by confirming observations on the Hale 5 m telescope at Palomar. During the following dark run at the Kitt Peak 4-m telescope, astrometry was obtained on 17 and 18 December. Astrometry on a single night was obtained on 20 January 2001 at the Palomar 5-m, as well as on 16 February on the 2.5-m Nordic Optical Telescope. Lastly, the object was imaged on 23 and 24 February using the ESO VLT UT-1 telescope. This brought the total observed arc to slightly more than one year, with extremely good time sampling in the recovery opposition. It is worth noting that without our March 2000 observations this object would have been 19 arcminutes away from its original ephemeris one year after discovery; it likely would not have been recovered without considerable effort, even with the large fields of view of mosaic cameras. Based on this experience, it seems plausible that some of the TNOs that are observed for only short arcs in their discovery opposition and then not found at their second opposition may very well have orbits similar to that of 2000 CR<sub>105</sub>. We thus take a fraction of 1 in  $\sim 400$  known TNO orbits as a lower limit to the number of 2000 CR<sub>105</sub>-like objects that have been detected in the flux-limited TNO/SDO database.

Based on its apparent *R*-band magnitude of  $m_R = 23.3 \pm 0.5$ , 2000 CR<sub>105</sub>’s diameter is roughly 400 km, based on an assumed 4% albedo. We do not consider our photometric data reliable enough, nor the assumed albedo accurate enough, to believe this to be accurate to more than a factor of two. This size places 2000 CR<sub>105</sub> at the high end of the known range of trans-neptunian objects, about a factor of two below the largest known

objects.

### 3 Orbit modelling

Using the available astrometric data, we have computed an osculating orbit solution taking into account the perturbations of the 4 giant planets (Table 1). We used the orbit determination software developed by Berstein and Khushalani (2000), optimized specifically for outer Solar System objects. This algorithm provides error estimates in the fitted osculating orbital elements (Table 2).

Based on the available data, 2000 CR<sub>105</sub>'s orbit is large, highly elliptical, and moderately inclined (Table 2). Its semimajor axis exceeds that of any other currently known multi-opposition TNO. 2000 CR<sub>105</sub> is currently 53 AU from the Sun and moving outwards, having passed perihelion in mid-1965. At pericenter the object would have been about 0.8 magnitudes brighter. The mean anomaly, argument of perihelion, and longitude of node are all well-determined. Overall this TNO might look like an outlier in the scattered disk distribution except for its very high  $q = 44$  AU perihelion (see Fig. 1). The perihelion distance has a fractional uncertainty much smaller than  $a$  because the  $a/e$  uncertainties are strongly correlated; the uncertainty in perihelion passage's distance is  $<1\%$ .

It is 2000 CR<sub>105</sub>'s exceptionally large perihelion distance which merits special attention. The only other SDO with a perihelion above 40 AU is 1995 TL<sub>8</sub> (Fig. 1), an object discovered by the Spacewatch program (Larsen *et al.* 2001).

## 4 Cosmogonic implications

In this section we present several possible scenarios for how 2000 CR<sub>105</sub> arrived on its current orbit. These include perihelion raising by diffusive chaos, as well as scattering due to (1) now-absent primordial embryos which passed through the forming Kuiper Belt, (2) a young Neptune that was forming a ‘fossilized scattered disk’, or (3) an unknown resident planetary-scale object in the distant Kuiper Belt.

### 4.1 Diffusive chaos

We have conducted a variety of numerical experiments to investigate the long-term dynamics of 2000 CR<sub>105</sub>. In the first of these we numerically integrated the best-fit orbit of this object, along with 20 other sets of initial conditions that are consistent with the observations at the  $1 - \sigma$  level. 2000 CR<sub>105</sub> and its “clones” were modelled as test particles moving in the gravitational field of the giant planets. The planetary positions and velocities came from the JPL DE403 ephemeris (with the terrestrial masses added to the Sun). The integration algorithm was the symplectic  $n$ -body map of Wisdom and Holman (1991), with a time step of 0.5 year. The integrations were for 5 Gyr of simulated time.

In addition to following the object trajectories, the tangent equations for each trajectory were also integrated (Holman and Murray 1996, Mikkola and Innanen 1999). This allows us to reliably estimate the rate at which nearby trajectories diverge from each other. Regular or quasi-periodic trajectories separate from each other linearly or at most polynomially with time. Chaotic motion is characterized by exponential divergence of neighboring trajectories; the time scale of this divergence is called the Lyapunov time.

All of the trajectories share a number of characteristics: (1) Each is chaotic with a Lyapunov time from  $5 \times 10^4$  to  $10^5$  years (15 to 30 orbital periods), consistent with previous studies of objects in this  $a, e$  regime (Torbett 1989, Torbett and Smoluchowski 1990). (2) the semimajor axis,  $a$ , oscillates rapidly within a series of discrete ranges. (3) The eccentricity,  $e$ , also varies rapidly; however, this variation is correlated with  $a$  in such a way that  $q$  varies much more smoothly. This occurs because the object receives an impulsive kick from Neptune as it passes perihelion; at each conjunction the position or perihelion distance of the object is nearly unaltered but the velocity, and thus  $a$  and  $e$ , is changed.

Fig. 2 shows a typical example of the evolution of  $a$  and  $q$  for one test particle. The rapid  $\sim 50$  Myr oscillation of  $q$  is caused by the “Kozai effect” of Neptune on the test particle (Kozai 1962), but its amplitude is far too low (see Thomas and Morbidelli 1996) to bring  $q$  down to small values. The center of each of the  $a$ -ranges, around which rapid oscillations occur, corresponds to a high-order mean-motion resonance with Neptune. This demonstrates the so-called phenomenon of “resonance sticking”. The resonance sticking seen proves that 2000 CR<sub>105</sub> is in or near a regime in which chaotic phenomena are operating and that this region of phase space may be connected to regions of lower perihelion by an extended chaotic zone; this suggests the possibility 2000 CR<sub>105</sub> was on a more ‘typical’ SDO orbit which then diffused via chaotic phenomena to its current high perihelion state.

The long time-scale variations of perihelion distance are important for evaluating the plausibility of this hypothesis. Of the 20 integrated particles, 2 diffused to a minimum

$q$  of 39 AU, although most remained between 42 and 47 AU (Fig. 3). We extended the integration of the test particle corresponding to the best-fit orbital elements to determine the long-term fate of this object; the “random walk” in  $q$  continued, with a maximum observed perihelion distance of  $q = 50$  AU. An orbit with  $q \sim 40$  AU was attained after 24 Gyr, at which point the semimajor axis diffused to very large ( $10^3$  AU) values. Shortly thereafter  $q$  dropped even lower, at which point the particle was ejected from the solar system by Neptune. The integrations demonstrate that particles in the estimated orbital region of 2000 CR<sub>105</sub> can, over very long time scales, reach perihelion distances at which strong scatterings due to Neptune occur. Of course, the opposite can occur because the equations of motion are time-reversible. The fact that none of the clones reached  $q=35$  AU on 5 Gyr time scales indicates that the probability of the reversed process of going to a state near that of 2000 CR<sub>105</sub> is low. In particular, the probability of leaving the vast chaotic zone to enter the slowly-diffusing regime is unconstrained; the absence of such trajectories in the Levison and Duncan (1997) simulations implies it is low. We briefly note that the TNO 1996 TL<sub>8</sub> is near a which might plausibly be reached by chaotic diffusion, but with a characteristic Lyapunov time longer than 20 orbital periods.

To accurately assess the probability of reaching the present orbit of 2000 CR<sub>105</sub> requires more extensive ‘forward’ numerical integrations of the formation of the scattered disk. However, an associated issue is to determine the origin of the dynamical chaos seen in the numerical integrations of 2000 CR<sub>105</sub> and its clones. To do so, we extended the work of Torbett (1989) and Torbett and Smoluchowski (1990). We integrated 5400 test particles trajectories for  $10^7$  years. We estimated the Lyapunov time of each trajectory, and based

on their histogram, we found that a value of 20 test-particle orbital periods separates those trajectories that are strongly chaotic from those that are not. As a test we checked that these high- $e$  test particles, when integrated without planetary perturbations, were not chaotic. In Fig. 1 we plot a point at those values of  $a$  and  $q$  for which the corresponding trajectory was chaotic with Lyapunov time less than 20 periods. The envelope of these points is, surprisingly, nearly a straight, sloped line. Based on earlier descriptions of the boundaries of the scattered disk chaotic zone, we expected to see chaos for trajectories with  $q$  below a fixed value (a horizontal dividing line); our results show that SDOs with large  $a$  can have large  $q$  and still exhibit chaos on orbital-period time scales. In Fig. 4 we plot initial  $a$  and  $e$  of those trajectories with estimated Lyapunov times shorter than 20 orbital periods. The solid line corresponds to the envelope of chaotic trajectories apparent on Fig. 1. Few chaotic trajectories are found below the line. The narrow ‘fingers’ of non-chaotic trajectories that extend above the line correspond to the stable islands of high-order mean-motion resonances with Neptune. These resonances are narrow but not microscopically so; at high  $e$  resonance widths do not depend as strongly on the order of the resonance as they do at low eccentricity. An analytic estimate of the width of the 6:1 mean motion resonance with Neptune, for example, yields roughly 3 AU at Neptune-crossing eccentricity (Morbidelli *et al.* 1995). On either side of the ‘fingers’ are chaotic regions resulting from the overlap of adjacent resonances. A detailed resonance overlap calculation, extending the work of Wisdom (1980), can be completed at high eccentricity by employing the technique of Ferraz-Mello and Sato (1989).

Malyshkin and Tremaine (1999) developed a 2-dimensional “keplerian map”, based on

the planar restricted three body problem, to study the long-term evolution of eccentric comet orbits perturbed by Neptune. Although their mapping assumes a fixed perihelion distance and models the entire gravitational interaction as an impulsive kick at perihelion passage, their results capture many of the features seen in our direct numerical integrations. Two of their principle results are: (1) the phase space is densely covered with chains of islands from mean-motion resonances, and (2) the chaotic zone between these islands is contiguous. That is, a trajectory can diffuse to arbitrarily large semimajor axis. Their first result we clearly see in our Fig. 4. Their second result is apparent in the small perihelion values attained by some of the 2000 CR<sub>105</sub> clones in our numerical integrations.

The details of our discussion can be refined once the semimajor axis of 2000 CR<sub>105</sub> is better determined, allowing us to determine exactly where in phase space it resides; it could conceivably be in a dynamically more stable region although this seems unlikely. Although we have given an extensive discussion of the diffusive chaos hypothesis (due to the fact that we can easily explore it numerically), the cosmogonic implications are even more dramatic if this hypothesis is either incorrect or untenable due to low probability. In such a case the existence of objects weakly coupled to the planetary system provides strong constraints on the formation of the outer Kuiper Belt. We now discuss three scenarios which could produce large numbers of such weakly-coupled or decoupled TNOs.

## 4.2 Primordial Embryos

Given that 4 planets with masses greater than 10 Earth masses formed in the outer Solar System, it is unlikely that no objects with martian-terrestrial mass also formed in the

region. Morbidelli and Valsecchi (1997) and Petit *et al.* (2000) developed the idea that one or several of these objects (which they call ‘embryos’) would have been logically scattered outward by Neptune and spent some time as SDOs transiting the forming Kuiper Belt, thus causing the dynamical excitation and mass loss observed therein. Close encounters with these passing embryos disturb the Kuiper belt out to the aphelic distance of the embryos, which are often 50-100 AU; scattering events can thus produce TNOs with perihelia well past Neptune on high- $e$  orbits. Once the embryos are eliminated by further gravitational interactions with Neptune, as 90% of SDOs are in 10 Myr (Duncan and Levison 1997), the TNOs remaining are extremely long-lived. In this scenario 2000 CR<sub>105</sub> may represent an object formed outside of 50 AU which was scattered to a large- $e$  orbit due to encounters with one of these embryos. Alternatively, 2000 CR<sub>105</sub> could have been formed much closer and *also* became a SDO via scattering by Neptune and then an encounter with a distant embryo sufficed to raise  $q$  to 44 AU.

### 4.3 Fossilized scattered disk

Thommes *et al.* (1999) propose that the ‘embryo’ passing through the Kuiper Belt may have been Neptune itself, during a formation process in which it transited the Kuiper belt on an orbit either more eccentric or with larger  $a$  before reaching its present nearly circular orbit at 30 AU. Being much more massive than the embryos discussed above, Neptune would be able to produce extensive dynamical ‘damage’ in a shorter time. With its current  $a$  and a modest  $e$  of  $\sim 0.3$ , which Thommes *et al.* damp via gravitational friction with a massive planetesimal disk in the vicinity, Neptune’s could encounter particles as far out

as 44 AU. After Neptune’s aphelion evolves out of the 40 AU region (presumably rapidly) the TNOs with  $q$  above this limit are ‘fossilized’ on orbits which either do not evolve over the lifetime of the solar system, or evolve only slowly via the diffusive mechanisms discussed above. 2000 CR<sub>105</sub> could be an example of the latter case. Because the furthest  $q$  of these objects will be just outside the largest  $Q$  of Neptune, the fossilized scattered disk forms an ‘arc’ in  $e/a$  space (see figures in Thommes *et al.* ) separated from a ‘cold disk’ (see Gladman 2001) by a gap in  $e$ .

#### 4.4 Resident planet

A last scenario is that 2000 CR<sub>105</sub> arrived in its current dynamical state due to gravitational interaction with a planetary-sized body that is *still resident* in the Kuiper Belt. This could come about in two ways. First, in the distant Kuiper belt, beyond the region sculpted by the whatever processes disturbed the 30-50 AU region, a planetary-mass body (the size of the moon to Mars for example), or several, may have formed *in situ* over the lifetime of the solar system and the perturbations of this body have sculpted the outer Kuiper belt. A Mars-sized body (with escape velocity of 5 km/s) at 100 AU where orbital velocities are only  $\sim 3$  km/s could scatter a body like 2000 CR<sub>105</sub> to its present orbit.

More likely may be a scenario in which several lunar—martian mass bodies were in the scattered disk, traversing in the 50–200 AU region. Many such bodies were likely formed interior to Neptune as the cores of the giant planets were accreting, and some would have ended up as SDOs. Since orbital velocities at those distances are comparable to the escape speeds of these bodies, mutual encounters between the ‘embryos’ could place one

or more of them on orbits entirely decoupled with Neptune; the planetary embryos still coupled to Neptune would have been rapidly destroyed, leaving the decoupled embryo(s) ‘lodged’ in the distant Kuiper belt. The resident embryo would then proceed to excite the orbital distribution, over the age of the Solar System, of the entire Kuiper Belt between its perihelion and aphelion distance. Similar ideas trace back to Fernández (1980) and Ip (1989), who sought to push short-period comets to Neptune-crossing orbits via decoupled embryos before long-term gravitational erosion was characterized as a supply process (Levison and Duncan 1997); we view the resident embryo scenario as potentially providing the ability produce objects like 2000 CR<sub>105</sub> and to remove many objects beyond the 2:1 resonance. Unpublished simulations by Morbidelli (2000, private communication) and Brunini (1999, private communication) show that this decoupling and ‘clearing out’ process can happen naturally. This scenario could be responsible for the apparent lack of objects on nearly circular orbits outside the 2:1 resonance (see Jewitt *et al.* 1998, Allen *et al.* 2000, and Gladman *et al.* 2001 for discussion) and the lack of detection of the so-called ‘Kuiper Wall’ (Trujillo 2000).

## 5 Conclusion

We estimate that the majority of the TNO surveys to date, searching within  $\sim 5^\circ$  of the ecliptic to limiting magnitude  $m_R=23-24$ , are capable of detecting 2000 CR<sub>105</sub> for  $< 1\%$  of its orbital period. Given this extreme detection bias against finding objects like 2000 CR<sub>105</sub>, there must be a large number of objects with perihelia higher than the 34–36 AU range for the scattered disk (used by Trujillo *et al.* 2000).

Thus, the ‘scattered disk’ may be much more massive than that component which is currently strongly coupled to Neptune, and likely merges into an ‘extended scattered disk’ where objects are only weakly coupled to Neptune. If the eccentricity and inclination distribution does not have the structure of a fossilized disk (with a gap in eccentricity) then it will be difficult to say where the ‘extended scattered disk’ ends! We propose that for the moment this object should *not* be classified as a scattered disk object unless a definition can be arrived at which would delineate SDOs from an object on a regular orbit (for example,  $a=210$  and  $e=0.7$ , which is neither chaotic nor coupled to Neptune, and yet clearly not a member of the cold disk. These nomenclature problems are expanded upon in Gladman (2001).

The lesson provided by our tracking of this exceptional TNO is that follow up inside the first year (2–3 months after discovery) is critical in order to detect these large orbits, for without such a recovery the TNO will be very far from even a ‘normal’ scattered orbit one year later, at which point recovery becomes difficult. It is difficult to estimate what fraction of previously-lost objects may have been similar to 2000 CR<sub>105</sub>; of the objects *already detected in the flux-limited sample*, (roughly 30 SDOs and/or  $\sim 400$  TNOs designated), the existence of 2000 CR<sub>105</sub> likely implies a strong lower limit of 5% of SDOs and  $\sim 0.2\%$  of TNOs to be on orbits like 2000 CR<sub>105</sub>, given the fraction of the TNOs that have had observations on only a single opposition.

We are not yet able to estimate the likelihood that 2000 CR<sub>105</sub> has diffused to a large  $q$  orbit if it was scattered to  $a \sim 200$  AU by Neptune. The rarity of similar particles in the integrations of Levison and Duncan (1996) may simply mean that this is rarer than  $\ll 1$  in

$10^3$  of the SDOs initially populating the scattered disk; the fraction of the SDOs *remaining* in this state after 5 Gyr will likely be roughly two orders of magnitude higher (Duncan and Levison 1996) and thus only 1 in  $10^5$  initial SDOs may need to reach the high- $q$  state. However, given the direct detection bias against, and the possible earlier loss of other already-discovered objects that may have been on similar orbits, the actual fraction of the visible trans-neptunian region that is also on high- $q$  orbits could be as large as several percent. In this case the diffusive hypothesis may become untenable and some of the more cosmogonically dramatic scenarios may be necessary. If a high- $a$  TNO totally decoupled from the planetary system can be identified then the reality of these dramatic scenarios can be constrained; the fact that the first high- $q$  TNO is in the diffusive boundary regime would then be understood to be due to detection bias which favors the latter's discovery. One cannot stress enough that continued tracking of *all* discovered TNOs, especially 2–3 months after discovery, is necessary in order to insure that additional interesting objects are not lost.

## 6 Acknowledgements

B. Gladman, J. Kavelaars, and M. Holman were visiting astronomers at the Canada France Hawaii telescope, operated by the National Research Council of Canada, le Centre National de la Recherche Scientifique de France, and the University of Hawaii. Data from VLT collected at the European Southern Observatory, Chile, proposals 66.C-0048A and 66.C-0029A. Observations at the Palomar Observatory were made as part of a continuing collaborative agreement between the California Institute of Technology and Cornell

University.

K. Aksnes, T. Grav, and M. Holman were visiting astronomers at the Nordic Optical Telescope. The Nordic Optical Telescope is operated on the island of La Palma jointly by Denmark, Finland, Iceland, Norway, and Sweden, in the Spanish Observatorio del Roque de los Muchachos of the Instituto de Astrofísica de Canarias. Some of the data presented here have been taken using ALFOSC, which is owned by the Instituto de Astrofísica de Andalucía (IAA) and operated at the Nordic Optical Telescope under agreement between IAA and the NBIfAFG of the Astronomical Observatory of Copenhagen.

M. Holman, B. Gladman, and T. Grav were visiting astronomers at the Kitt Peak National Observatory, National Optical Astronomy Observatory, which is operated by the Association of Universities for Research in Astronomy, Inc. (AURA) under cooperative agreement with the National Science Foundation.

This work was supported in part by an ACI Jeune grant from the French Ministry of Research, and NASA grants NAG5-10365 and NAG5-9678 to the Smithsonian Astrophysical Observatory.

We thank Joe Burns, Brian Marsden, Alessandro Morbidelli, and Norm Murray for helpful input.

## References

- Allen, L., Bernstein, G., and Malhotra, R. 2001. The edge of the solar system. *Ap. J. Lett.* **549**, 241–244.
- Bernstein, G. and Khushalani, B. 2000. Orbit Fitting and Uncertainties for Kuiper Belt Objects. *A. J.* **120**, 3323–3332.
- Dones, L., H. F. Levison, and M. Duncan 1996. On the dynamical lifetimes of planet-crossing objects. In *Completing the Inventory of the Solar System* (T. W. Rettig, J. Hahn Eds.), Astronomical Society of the Pacific Press, Vol. 107, pp. 233–244.
- Dones, L., Gladman, B., Melosh, H. J., Tonks, W. B., Levison, Harold F., Duncan, M. 1997. Dynamical Lifetimes and Final Fates of Small Bodies: Orbit Integrations vs Opik Calculations. *Icarus* **142**, 509–524.
- Duncan, M., Quinn, T., Tremaine, S. 1987. The formation and extent of the solar system comet cloud. *A. J.* **94**, 1330–1338.
- Duncan, M. J., Levison, H. F. (1997) A scattered comet disk and the origin of Jupiter family comets. *Science* **276**, 1670–1672.
- Ferraz-Mello, S., Sato, M. 1989. The very-high-eccentricity asymmetric expansion of the disturbing function near resonances of any order. *Astronomy and Astrophysics* **225**, 541–547.
- Gladman, B. 2001. Nomenclature in Kuiper Belt, in *Proceedings of Joint Discussion 4 of the 2000 IAU General Assembly*. (A. Lemaitre Ed.) Kluwer, in press.
- Gladman, B., Kavelaars, J., Petit, J-M., Morbidell, A., Holman, M., Loredó, T. 2001. The

- Structure of the Kuiper Belt: Size Distribution and Radial Extent. A.J., submitted.
- Jewitt, D. G., Luu, J., and Chen, J. 1996. The Mauna Kea-Cerro-Tololo Kuiper Belt and Centaur Survey. *A. J.* **112**, 1225-1238.
- Jewitt, D. G., Luu, J., and Trujillo, C. 1998. Large Kuiper Belt objects: The Mauna Kea 8K CCD survey. *A. J.* **115**, 2125-2135.
- Larsen, J. A., Gleason, A. E., Danzl, N. M., Descour, A. S., McMillan, R. S.; Gehrels, T., Jedicke, R., Montani, J. L., Scotti, J. V. 2001. The Spacewatch Wide-Area Survey for Bright Centaurs and Trans-Neptunian Objects. *Astron. J.* **121**, 562-579.
- Levison, H. F., Duncan, M. J. 1997. From the Kuiper Belt to Jupiter-Family Comets: The Spatial Distribution of Ecliptic Comets. *Icarus*, **127**, 13-32.
- Malyshkin, L., Tremaine, S. 1999. The Keplerian Map for the Planar Restricted Three-Body Problem as a Model of Comet Evolution. *Icarus*, **141**, 341–353.
- Mikkola, S., Innanen, K. 1999. Symplectic Tangent map for Planetary Motions *Celest. Mech. Dyn. Astron.* **74**, 59–67.
- Millis, R. L., Buie, M. W., Wasserman, L. H., Elliot, J. L., Kern, S. D., Wagner, R. M. 2000. The Deep Ecliptic Survey. *B.A.A.S.* **vol**, ??
- Morbidelli, A., Thomas, F., Moons, M. 1995. The resonant structure of the Kuiper belt and the dynamics of the first five trans-Neptunian objects. *Icarus*, **118**, 322–340.
- Morbidelli, A. and Valsecchi, G. 1997, NOTE: Neptune Scattered Planetesimals Could Have Sculpted the Primordial Edgeworth-Kuiper Belt. *Icarus*, **128**, 464.
- Petit, J-M., Morbidelli, A. and Valsecchi, G. 1999. Large Scattered Planetesimals and the Excitation of the Small Body Belts. *Icarus*, **141**, 367.

- Torbett, M. 1989. Chaotic motion in a comet disk beyond Neptune: The delivery of short-period comets. *A.J.* **98** 1477-1481.
- Torbett, M. and Smoluchowski, R. 1990. Chaotic motion in a primordial comet disk beyond Neptune and comet influx to the solar system. *Nature*, **345**, 49–51.
- Thomas, F., and A. Morbidelli (1996) The Kozai resonance in the outer solar system and the dynamics of long-period comets *Celest. Mech.*, **64**, 209–229.
- Thommes, E., Duncan, M., Levison, H.F. 1999. The formation of Uranus and Neptune in the Jupiter-Saturn region of the Solar System. *Nature*, **402**, 635–638.
- Trujillo, C. 2000. Simulations of the bias effects in Kuiper Belt surveys. in *Minor Bodies in the Outer Solar System* (A. Fitzsimmons, D. Jewitt, R.M. West, Eds.) pp. 109–115. Springer-Verlag, Berlin.
- Trujillo, C., D. Jewitt, Luu, J. 2000. Population of the Scattered Kuiper Belt *Ap. J.* **102**, 529–533.
- Wisdom, J. 1980. The resonance overlap criterion and the onset of stochastic behavior in the restricted three-body problem. *Astron. J* **85**, 1122-1133.
- Wisdom, J., Holman, M. 1991. Symplectic maps for the n-body problem. *A. J.* **102**, 1528–1538.

**Table 1. Astrometric observations and calculated orbit for 2000 CR<sub>105</sub>**

Object	UT Date	$\alpha(2000)$	$\delta(2000)$	R	Obs.	Note
	yyyy mm dd.ddddd	hh mm ss.ss	dd mm ss.s	mag	Code	
K00CA5R	2000 02 06.30637	09 14 02.39	+19 05 58.7	22.5 R	695	1
K00CA5R	2000 02 06.43541	09 14 01.90	+19 06 01.4		695	1
K00CA5R	2000 02 27.12907	09 12 44.37	+19 13 04.6	23.0 R	695	1
K00CA5R	2000 02 27.22612	09 12 43.98	+19 13 06.3		695	1
K00CA5R	2000 03 28.38346	09 11 17.68	+19 20 37.4		568	2
K00CA5R	2000 03 28.40927	09 11 17.63	+19 20 37.6		568	2
K00CA5R	2000 03 28.43164	09 11 17.59	+19 20 37.9		568	2
K00CA5R	2000 03 29.23055	09 11 15.99	+19 20 46.3		568	2
K00CA5R	2000 03 29.25196	09 11 15.95	+19 20 46.5	23.1 R	568	2
K00CA5R	2000 03 29.27248	09 11 15.91	+19 20 46.7	23.4 R	568	2
K00CA5R	2000 11 24.30080	09 22 07.39	+18 49 14.6		809	3 *
K00CA5R	2000 11 25.30941	09 22 06.97	+18 49 25.1		809	3 *
K00CA5R	2000 11 27.48283	09 22 05.77	+18 49 49.1	23.5 R	675	4
K00CA5R	2000 11 27.54557	09 22 05.73	+18 49 49.1	23.7 R	675	4
K00CA5R	2000 11 28.48968	09 22 05.11	+18 49 59.8	24.1 R	675	4
K00CA5R	2000 11 28.52381	09 22 05.08	+18 50 00.3	23.6 R	675	4
K00CA5R	2000 12 17.45692	09 21 38.68	+18 54 34.5	23.0 R	695	5
K00CA5R	2000 12 17.49240	09 21 38.62	+18 54 34.9	23.2 R	695	5
K00CA5R	2000 12 17.53331	09 21 38.54	+18 54 35.9	23.4 R	695	5
K00CA5R	2000 12 18.43274	09 21 36.63	+18 54 51.1	23.0 R	695	5
K00CA5R	2000 12 18.50613	09 21 36.52	+18 54 52.2	22.8 R	695	5 *
K00CA5R	2001 01 20.39079	09 19 58.51	+19 06 04.4	23.1 R	675	6
K00CA5R	2001 01 20.39910	09 19 58.46	+19 06 04.6		675	6
K00CA5R	2001 01 20.46716	09 19 58.24	+19 06 06.2	23.1 R	675	6
K00CA5R	2001 02 15.99209	09 18 17.96	+19 15 46.4	23.7 R	950	7
K00CA5R	2001 02 16.03317	09 18 17.80	+19 15 47.2	23.4 R	950	7
K00CA5R	2001 02 16.08746	09 18 17.59	+19 15 48.4	23.5 R	950	7
K00CA5R	2001 02 23.15703	09 17 51.48	+19 18 11.2	23.3 R	309	8
K00CA5R	2001 02 24.24770	09 17 47.52	+19 18 32.4		309	8

Notes: 1 – Millis *et al.* KPNO 4-m and WIYN (MPEC 2000-F07)

2 – Gladman, Kavelaars, Holman, Petit (CFHT-3.5m); 3 – Gladman (ESO-2.2m);

4 – Nicholson, Kavelaars (Palomar-5m); 5 – Holman, Gladman, Grav (KPNO-4m);

6 – Nicholson, Gladman (Palomar-5m); 7 – Grav, Holman (NOT-2.5m);

8 – Gladman (VLT UT1-8m)

Astrometric uncertainties  $\alpha \pm 0.03s$  ,  $\delta \pm 0.4''$  except \* for which  $\alpha \pm 0.07s$  ,  $\delta \pm 1''$ .

Photometric uncertainties  $\pm 0.5$  mag

**Table 2. Orbital elements for 2000 CR<sub>105</sub>**

Orbital element (J2000)	Value	1-sigma error
semimajor axis $a$	216 AU	9 AU
eccentricity $e$	0.795	0.010
<b>perihelion distance <math>q</math></b>	44.2	0.3 AU
inclination $i$	22.759°	0.002°
longitude of node $\Omega$	128.287°	0.001°
argument of pericenter $\omega$	317.0°	0.6°
Date of pericenter passage (JD)	2438870	70
mean anomaly $M$	3.9°	0.2°

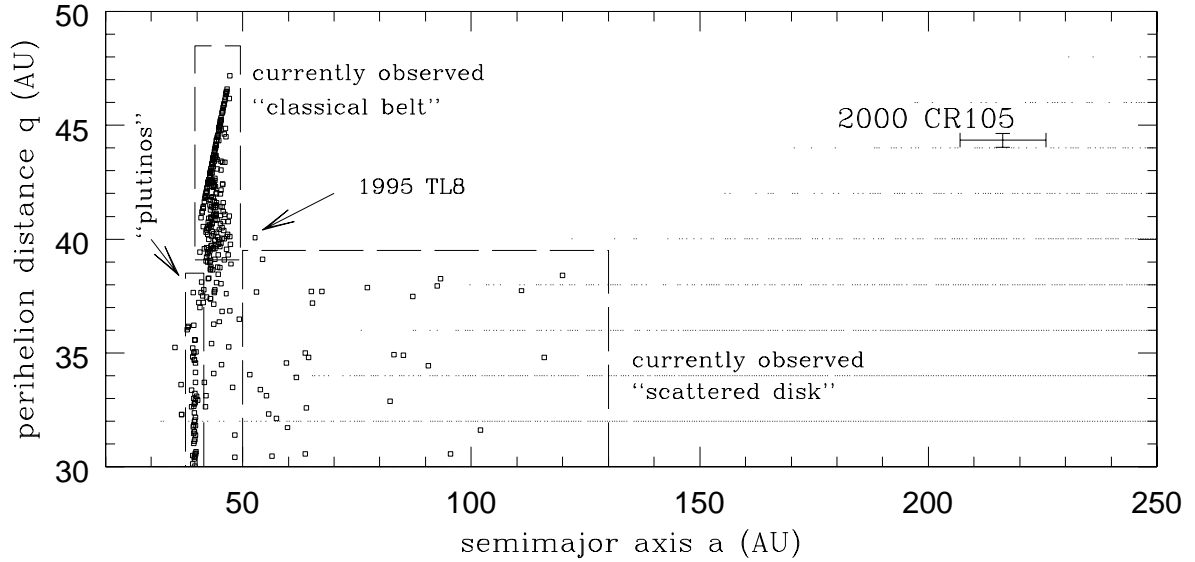


Figure 1: Squares indicate estimated semimajor axes and perihelion distances for all trans-neptunian objects in the Minor Planet Center database as of February 2001. Very approximate boundaries for membership in the classical Kuiper Belt, plutino population, and scattered disk are indicated (only to guide the eye). Small points indicate that a numerical integration (see text) showed a chaotic orbital evolution for an orbit with those initial conditions. Note that there are severe detection biases in this plot and it is not a representative sampling of the trans-neptunian region.

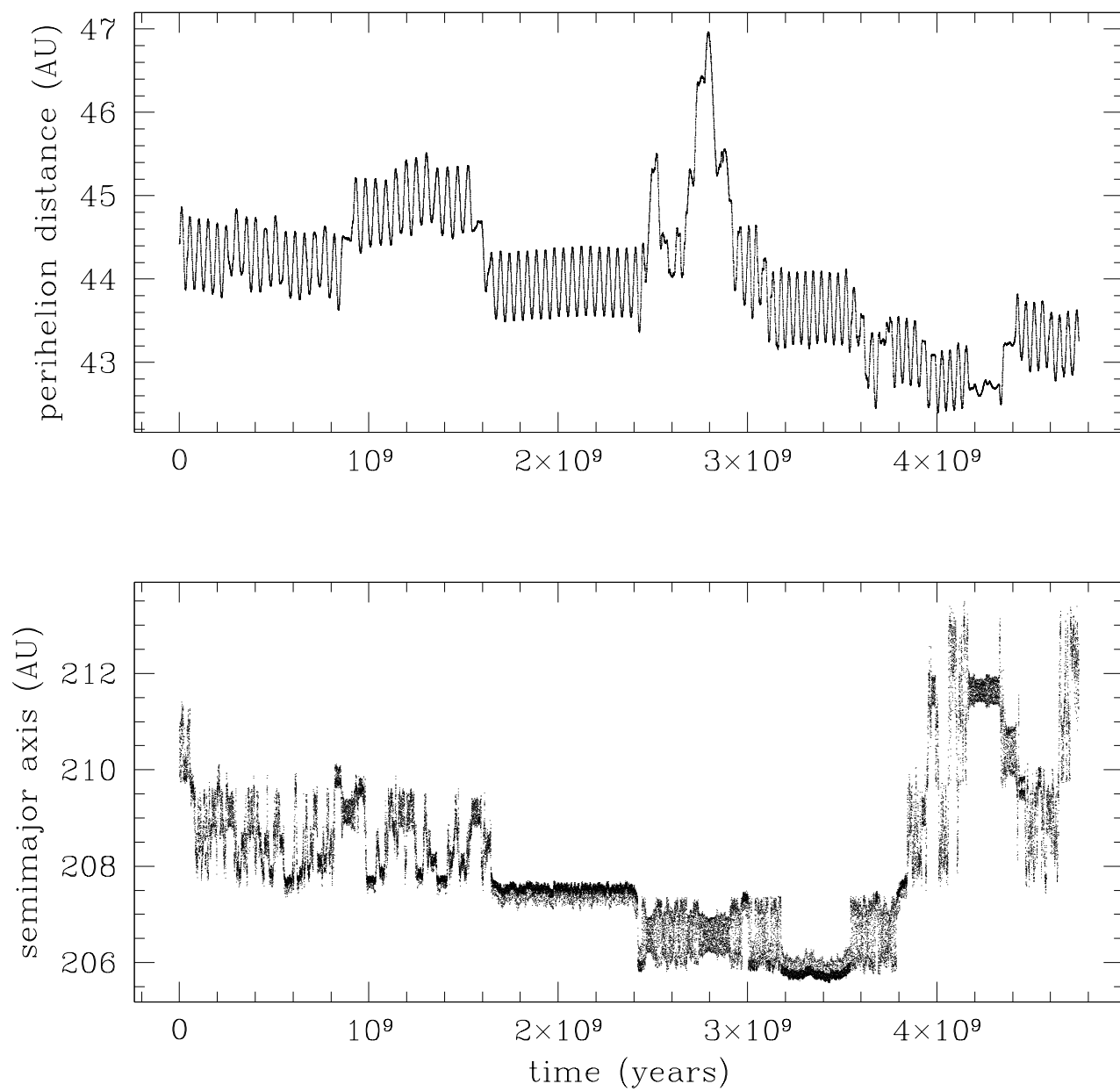


Figure 2: The evolution for the semimajor axis  $a$  and pericentric distance  $q$  for a test particle integrated with an initial orbit consistent with that of 2000 CR<sub>105</sub>. See text for discussion.

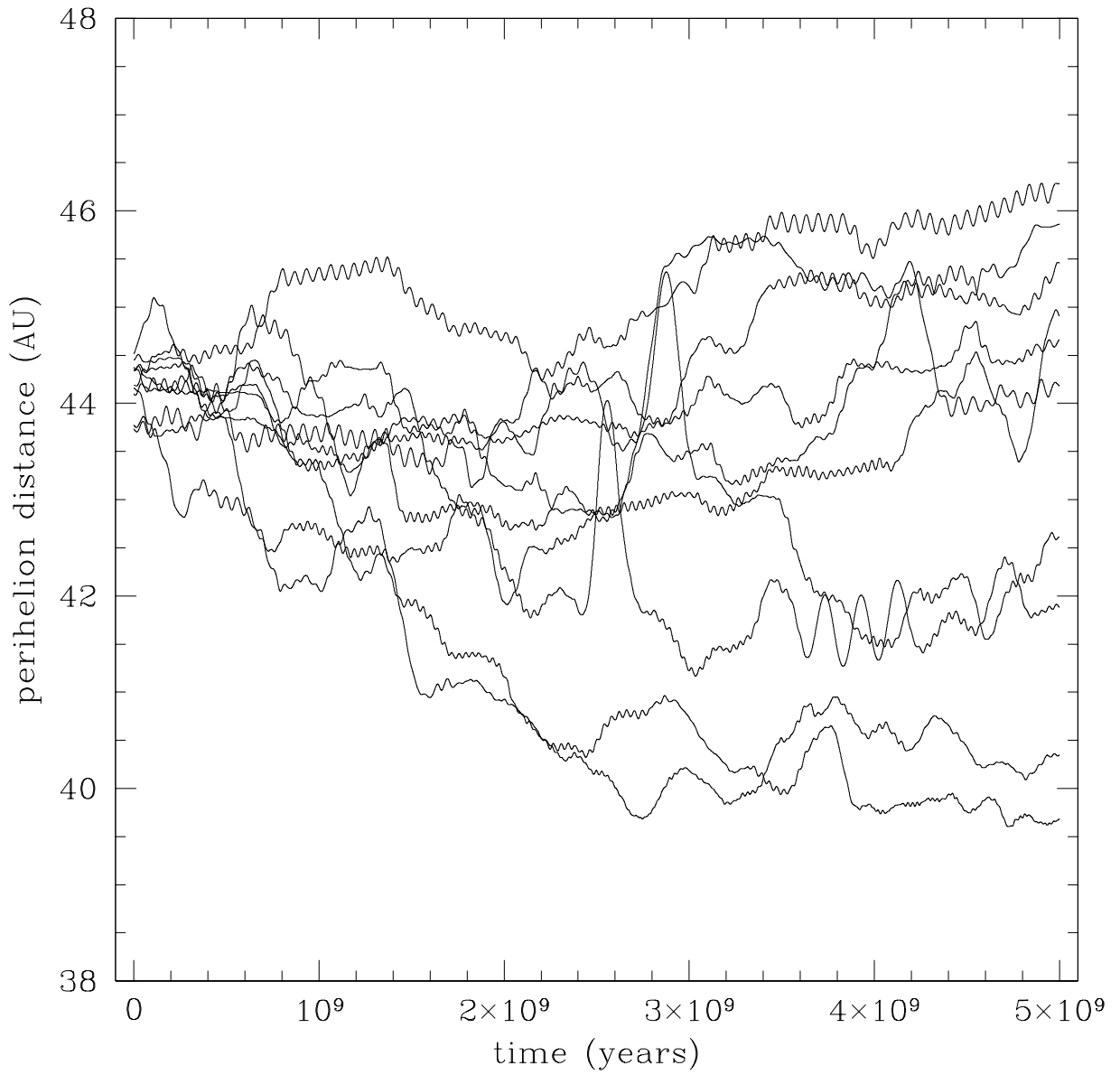


Figure 3: The  $q$ -evolution for 10 of the 20 integrated ‘clones’, showing the range of variation for particles consistent with our best-fit orbit for 2000 CR<sub>105</sub>.

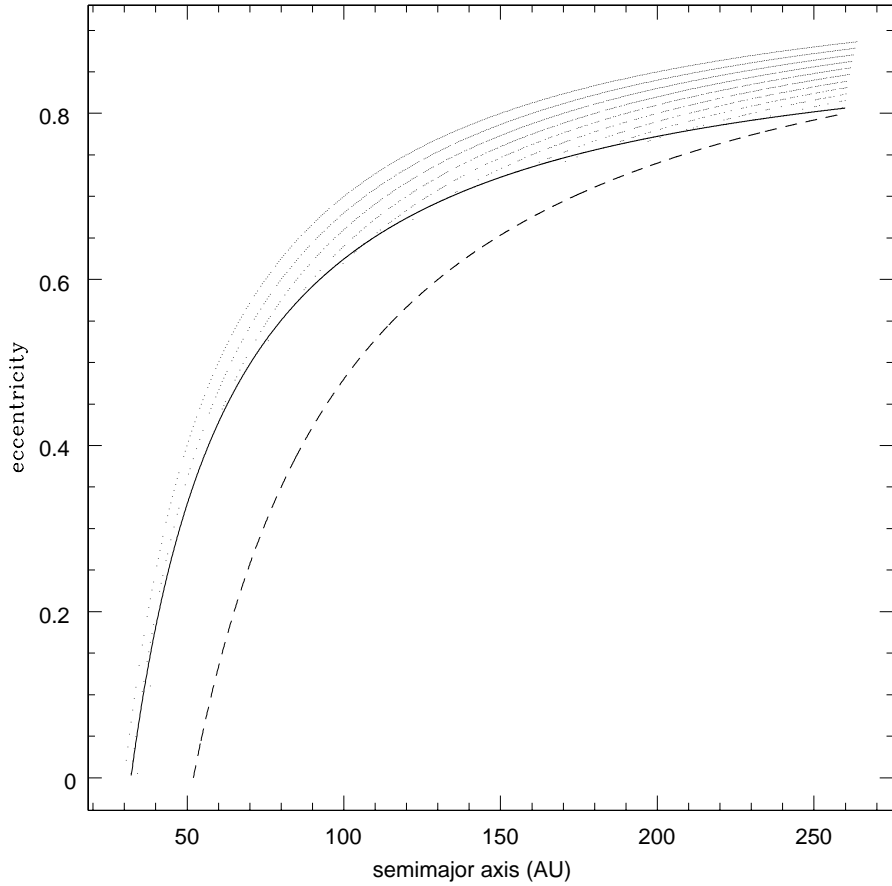


Figure 4: An illustration of the chaotic structure of the region of large- $a$  solar system orbits. Initial conditions were  $a=30\text{--}260$  AU with  $e$  selected to sample  $q=30\text{--}52$  AU in increments of 2 AU. For the remaining elements we chose inclination  $i = 17^\circ$ , longitude of ascending node  $\Omega = 0^\circ$ , argument of perihelion  $\omega = 0^\circ$ , and mean anomaly  $M = 0^\circ$ , with respect to the DE403 ecliptic and equinox. Each dot corresponds to an integrated trajectory (see text) with Lyapunov time shorter than 20 of its orbital periods. The solid line denotes the relation  $q = 30 + 0.09(a - 30)$  (determined empirically) which roughly bounds the envelope of chaotic trajectories (also see Figure 1). Above this line, most of the trajectories exhibit strong, short time-scale chaos. The dashed line denotes the lower eccentricity boundary of the integrated trajectories. Between the dashed line and the solid line few of the trajectories exhibited short time-scale chaos. The ‘fingers’ of regular regions at large  $a$  (absence of dots), reaching to higher values of  $e$ , correspond to the stable regions associated with individual mean-motion resonances.